# OXIDE DISPERSION STRENGTHENED (ODS) STEELS FOR CANDU SUPERCRITICAL WATER-COOLED REACTOR (SCWR) FUEL CLADDING

**S. Kuyucak, B. Shalchi Amirkhiz and C. Tesone**

CanmetMATERIALS, Hamilton, Ontario, Canada

Selcuk.Kuyucak@Canada.ca, Babak.Shalchi_Amirkhiz@Canada.ca, Carlo.Tesone@Canada.ca

## Abstract

ODS steels incorporate nano-sized yttrium titanate particles for improved high temperature strength. It's a unique strengthening mechanism for imparting good creep resistance to ferritic steels. Together with their low neutron absorption cross-section and good corrosion and SCC resistance, ferritic ODS steels are ideal candidates for SCWR fuel cladding material. ODS steels were prepared by mechanically alloying Fe-14Cr-Mo or W (wt. pct.) pre-alloyed steel powders with nano-sized yttria and titanium powder in a lab-sized attritor in 2-3 kg batches. The milled powders were retrieved from the attritor and placed in thick-wall containers under inert atmosphere, degassed at 400°C, sealed into composite billets, aged at 800°C and consolidated by extrusion at 900-1100°C. The resulting steel rods were characterized by advanced electron microscopy and mechanical testing. Hardness surveys conducted along the length of the rods showed high hardness (450 HV) when even dispersion strengthening was obtained; however, some rods were interspersed with transition to low hardness areas.

## 1 Introduction

Canada's participation to Generation IV International Forum (GIF) has culminated in a pressure-tube based supercritical water-cooled reactor (SCWR) design. Availability of key structural materials to construct in-core components is critical to realizing this design. In this respect, fuel cladding presents the greatest challenge because of its very high surface temperature, expected to reach up to 825°C in the hot zone. SCWR environment demands high temperature creep-, irradiation-, and corrosion- resistance. A 3.5 year component life is required for a typical fuel-cladding in the Canadian conceptual design. Oxide dispersion strengthened (ODS) steels via mechanical alloying hold a promise. ODS imparts high temperature creep- and radiation- resistance. Recent work in super-critical water (SCW) loop also showed moderate improvements in corrosion-resistance.

Work on ODS steels mostly focused on ferritic / martensitic (F/M) and ferritic steels, as these steels have the most promising radiation and stress-corrosion cracking (SCC) resistance, and very favourable neutron-cross section for high reactor efficiency. They do not, however, possess high temperature strength but can be strengthened by oxide dispersion for creep resistance. The chromium level in ferritic steels is limited typically to 14% or less to avoid

Table 1. Steels studied for ODS processing; compositions in wt. pct. and size distributions after nitrogen gas atomization.

| Steel Type | Heat No. | C | Cr | Mo | W | Si | Mn | Ni | S | N | |
|---|---|---|---|---|---|---|---|---|---|---|---|
| | | | | | | | | | | (1) | (2) |
| MA957 | V9011 | 0.022 | 13.1 | 0.32 | - | <0.01 | 0.057 | <0.01 | 0.0030 | 0.012 | 0.026 |
| 14YWT | V0003 | 0.016 | 14.4 | - | 2.1 | 0.027 | <0.05 | 0.37 | 0.0040 | 0.016 | 0.030 |
| F/M steel | V0004 | 0.11 | 11.9 | - | 2.2 | 0.035 | <0.05 | 0.33 | 0.0020 | 0.017 | 0.031 |

Others: 0.001 Al, <0.005 P. Nitrogen: (1) before, (2) after gas atomization.

| Steel Type | Heat No. | Wt. pct. under the indicated size in μm | | | | | | | $d_{50\%}$ (μm) |
|---|---|---|---|---|---|---|---|---|---|
| | | -212 | -150 | -106 | -75 | -63 | -53 | -45 | |
| MA957 | V9011 | 96.0 | 90.1 | 80.3 | 66.0 | 57.0 | 48.8 | 40.4 | 55 |
| 14YWT | V0003 | 96.8 | 91.6 | 82.3 | 68.3 | 59.0 | 50.8 | 42.4 | 53 |
| F/M steel | V0004 | 91.8 | 80.1 | 65.2 | 49.5 | 41.7 | 35.5 | 29.2 | 75 |

embrittlement caused by the formation of FeCr-ordered σ-phase during service [1]. Ferritic steels, being non-transforming, can also suffer from high anisotropy following consolidation by extrusion, with poorer properties in the radial and hoop directions [2]. F/M steels are less corrosion resistant because of their lower Cr-content to stay within the gamma-loop, but they are transformable and can be normalized to remove their process induced anisotropy. Their corrosion resistance can be improved by surface coatings.

Oxide dispersion strengthening in steels specifically refers to the processing by high-energy milling of steel powders with nano-sized yttria particles in the presence of titanium powder. Observations by advanced analytical techniques such as atom probe microscopy / tomography have shown that, during high-energy ball milling, yttria particles dissociate and go into solid solution as supersaturated yttrium and oxygen atoms in the ferrite matrix [3]. These then re-precipitate on aging at 400 - 1150°C as yttrium titanate clusters, which are typically an order of magnitude smaller than the original yttria powder, and provide the observed dispersion strengthening of ferrite [4,5]. Importance of having dissolved titanium in refining the oxide nano-clusters was first recognized by Ukai in Japan [6], its presence in the oxides also significantly decreases their coarsening above 1000°C [7,8]. These clusters were shown to range from non-equilibrium sub-oxides similar to coherent GP-zone transition phases to stoichiometric oxides, depending on the thermal history of the steel [9-12]. Steels and coatings alloyed with yttrium form a very adherent protective yttria layer stable at high temperatures, possibly due to a special orientation relationship with the parent steel matrix. It is suspected that yttria works well as a dispersion agent for the same reason.

Fig. 1. Mechanical alloying facility (attrition mill and degassing unit) set up to process ODS steels.

## 2 Experimental

### 2.1 Powder Preparation

Ferritic (MA957 and 14WYT) and Ferritic / Martensitic (F/M) steels were selected for study. The pre-alloyed steels were prepared in CanmetMATERIALS (CMAT) and sent to Atomization Systems Ltd. UK, for remelting and nitrogen gas atomization. The steels were induction melted in 150 kg batches and poured through a clay-graphite crucible tundish fitted with a 5 mm ID nozzle. The steel velocity was controlled by its head height in tundish, and the nitrogen gas flow-rate was kept at 4 $Nm^3$ per kg steel processed. The powders were sieved and sized. Their compositions and size distributions are given in Table 1. The steel powders in the size range of -150 / +45 μm were used for ODS steel processing.

Nitrogen uptake by the steel powders on atomization was modest; the final nitrogen contents were about 0.03 pct. Only 0.1 pct. Ti would be needed in fixing this as TiN. Sufficient excess titanium was added to form yttrium titanates and titanium nitrides.

Plasma atomised, commercial purity Titanium powder with 0.0030 pct. N and in the size range of -106 / +45 μm, was procured from Advanced Powders and Coatings. Nano-sized yttria powder was procured from China, its Average Particle Size (APS) was confirmed by TEM as 30 ±10 nm [13].

### 2.2 Mechanical Alloying

A mechanical alloying facility was set up to process the steel powders consisting of a water-cooled high-energy ball mill (Lab. Attritor 1-SD from Union Process, Ohio), a degassing station with a turbomolecular pump and tube furnace to degas canned powders, and a glove

Table 2. Milled powders for consolidation into ODS steels.

| Powder | Steel Type | Powder Batch, (kg) | Yttria (wt. pct.) | Grinding Ratio | Milling Time (h) | Surfactant |
|---|---|---|---|---|---|---|
| M1 | MA957 | 2.840 | 0.50 | 10 | 4 | - |
| M2 | MA957 | 2.840 | 0.40 | 10 | 8 | - |
| M3 | MA957 | 2.840 | 0.35 | 10 | 12 | - |
| M4 | 14YWT | 2.840 | 0.35 | 10 | 24 | Methyl alc., 9 mL/kg |
| M5 | 14YWT | 1.925 | 0.38 | 14.8 | 48 | Methyl alc., 10 mL/kg |
| M6 | F/M steel | 1.900 | 0.35 | 15 | 48 | TEA, 2.6 mL/kg |
| M7 | F/M steel | 1.900 | 0.42 | 15 | 48 | TEA, 2.6 mL/kg |
| M8 | MA957 | 1.900 | 0.53 | 15 | 48 | TEA, 1.3 mL/kg |
| M9 | 14YWT | 1.900 | 0.52 | 15 | 48 | TEA, 1.3 mL/kg |
| ORNL | 14YWT | 2.500 | 0.50 | 11.4 | 48 | - |

Note: TEA is Tri-ethanol-amine.

box for handling milled powders under inert atmosphere (Fig. 1). The ball mill had a 9.5 L tank with a 60% (5.7 L) working volume to take 27 kg grinding media (3/16" dia. 440C stainless steel balls). The milling action was provided by a rotating vertical shaft with horizontal impellers. The grinding ratio (media to powder ratio by volume) was kept at 10:1 to 15:1 to process 2 – 3 kg powder per batch under an argon atmosphere. The mill was operated at an average speed of 300 rpm for 24 to 48 h under an argon atmosphere. The milled powders were discharged under argon and kept in a glove box. They were subsequently placed in thick-walled mild steel containers, degassed at 400°C to 1 μbar pressure via ¼" dia. nickel tubing in 2 – 3 days, and hermetically sealed by crimping and welding to form composite billets. Powder consolidation was carried out by extrusion at 850 – 1150°C with an extrusion ratio of 4 - 6. During reheating, billets were aged at 800°C for 2 h to allow the precipitation of yttrium titanates, prior to reaching the soaking temperature.

Table 2 shows the batches of milled powders obtained. The steel powders were pre-mixed with the indicated amount of yttria and 0.9 wt. pct. titanium powder in a lab. mixer prior to charging to the mill. In some batches, a small amount of surfactant was added to improve the dispersion of yttria in the mixture.

The first four batches were made to investigate the effect of milling time on the evolution of steels' microstructure; otherwise the milling continued for 48 h to ensure complete dispersion of yttria. The grinding ratio was kept at 10 – 15. The milling was carried out at CMAT's

vertical shaft ball mill, except one batch was made at Oak Ridge National Laboratory, TN, where milling was carried out in a horizontal shaft mill made by Zoz, Germany.

### 2.3 Powder Consolidation by Extrusion

Table 3 shows milled powders consolidated into extruded rods. Samples from the first five batches of milled powders were placed in 150 mm long, 68 mm OD, 10 mm wall, steel cans; degassed and sealed. CMAT's extrusion facility was not yet set up due to lab. relocation from Ottawa to Hamilton, so these were extruded at a Canadian industrial facility using their 200 t machine and fibre glass lubricant.

Subsequent extrusions were carried out at CMAT's Macrodyne press with a 450 t closing force, at higher extrusion ratios. For extrusion temperatures at 950°C and above, fiber glass lubricant; below 950°C, copper sheath lubricant, were used. Container and tooling were kept at 400°C. Extrusion speed was 34 mm/s.

## 3 Results and Discussion

### 3.1 Yttria Requirement for Mechanical Alloying

In ODS steel processing, the powders are pre-mixed in a lab. mixer, then mechanically alloyed in an attrition mill. In this process, yttria first coats the steel powder, then becomes embedded in the steel by the action of mechanical alloying. During pre-mixing, the nano-sized yttria coats the steel powders' surface. Ideally, at least a mono-layer of yttria should be present on steel surface. The required yttria content can be calculated by comparing the surface area of an average sized steel particle to the number of yttria particles that can be fitted on that surface:

$$n_{\mathrm{Y}} = \frac{\pi D_{\mathrm{Fe}}^2}{\frac{\pi}{4} D_{\mathrm{Y}}^2} \tag{1}$$

$$g_{\mathrm{Y}} = \frac{n_{\mathrm{Y}} \rho_{\mathrm{Y}} V_{\mathrm{Y}}}{\rho_{\mathrm{Fe}} V_{\mathrm{Fe}}} = 4 \frac{\rho_{\mathrm{Y}} D_{\mathrm{Y}}}{\rho_{\mathrm{Fe}} D_{\mathrm{Fe}}} \tag{2}$$

$$IPS_{\mathrm{Y}} = \sqrt[3]{\frac{\pi}{24} D_{\mathrm{Fe}} D_{\mathrm{Y}}^2} \tag{3}$$

where:

| | | | |
|---|---|---|---|
| $n$ | number of powder particles | Fe | subscript for steel |
| $D$ | average diameter of a powder particle (μm) | Y | subscript for yttria |
| $V$ | volume of an average dia. particle (μm$^3$) | | |
| $\rho$ | density (kg/L) | | |
| $g$ | mass fraction (wt. pct.) | | |
| $IPS$ | Interparticle spacing (μm) | | |

Table 3. Milled steel powders consolidated into extruded rods.

| Extruded Rod | Steel | Extrusion Ratio[a] | Temp. of Ext., °C | Y-added wt. pct. | Y-ICP[b] wt. pct. | Die dia. mm | Rod Length, in. | Hardness HV | Comments |
|---|---|---|---|---|---|---|---|---|---|
| N1A | MA957 | 4.0 | 1150 | 0.39 | 0.37 | 34 | 18.3 | 157 | |
| N2A | " | " | 1150 | 0.32 | 0.34 | " | 18.1 | 153 | |
| N3A | " | " | 1150 | 0.28 | 0.0001 | " | 20.7 | 152 | |
| N4A | 14YWT | " | 1150 | 0.28 | | " | 20.1 | 145 | |
| N5A | " | " | 1150 | 0.30 | 0.0002 | " | 19.3 | 156 | |
| N5B | " | 4.5 | 1150 | 0.30 | 0.0000 | 32 | 21.6 | 154 | |
| M1B | MA957 | 6.45 | 875 | 0.39 | 0.0000 | 25 | 3.5 | 160 | Back-extruded, discarded |
| M3B | " | " | 875 | 0.28 | 0.0014 | " | 4.5 | 159 | Back-extruded, discarded |
| M4B | 14YWT | 6.05 | 912 | 0.28 | | " | 25.5 | 155 - 380 | Showed transition [d] |
| M6A-1 | F/M steel | " | 865 | 0.28 | | " | 6 | 560 / 490[c] | Stalled after a short extrusion |
| M6A-2 | " | " | 950 | 0.28 | | " | 11 | 580 | Remaining billet extruded |
| M7A | " | 6.45 | 925 | 0.33 | 0.43 | " | | 130 | |
| M7B | " | 6.05 | 915 | 0.33 | | " | 22 | 155 - 618 | Showed transition [d] |
| M9A-1 | 14YWT | " | 900 | 0.33 | | " | 2 | 160 | Stalled after a short extrusion |
| M9A-2 | " | " | 950 | 0.41 | | " | 22.5 | 473 | Remaining billet extruded |
| ORNL | " | " | 1100 | 0.41 | | " | 13.5 | 165 | Stalled at 950°C. Re-extruded. |

Nomenclature: Prefix "N" denotes billets extruded at an industrial site; "M", by Macrodyne at CMAT. The second digit refers to the mechanical alloying batch number. Billets prepared from each batch of milled powder were sequenced as A, B, etc. Notes: [a] Extrusion Ratio: billet area to area of die opening. [b] wet-chemical analysis of Y in steel shavings by SGS Labs using inductively-coupled plasma (ICP) spectroscopy. [c] Hardness before and after tempering (single values, before tempering). [d] Showed transition from soft to hard matrix.

Table 4. Yttria requirement from steel and yttria powder properties.

| | Steel | $Y_2O_3$ | |
|---|---|---|---|
| Density (kg/L) | 7.9 | 5.01 | |
| Average Particle Size (μm) | 50 | 0.020 | 0.030 |
| Mass fraction of yttria to build a monolayer | | 0.10% | 0.15% |
| Number density (per $\mu m^3$) | | 382 | 170 |
| Average interparticle spacing (μm) | | 0.14 | 0.18 |

Table 4 shows the calculated amount of yttria to build a monolayer over steel particles and the resulting inter-particle spacing of yttria within the steel matrix for a uniform distribution. As seen, only 0.10 to 0.15% yttria is required. More yttria can be added, but if yttria particles clump together and not disperse into the steel, they will form pockets of weakness. It is thus customary to limit the yttria additions to 0.3 - 0.5%, depending on the particle size of the mixture. Fig. 2(a) shows a typical yttria coverage on steel powder surface on pre-mixing. It was very difficult to disperse "excess" yttria by dry mixing. Macroscopically, streaks of yttria did not disappear even after long mixing times, Fig. 2(b). Surfactants, such as tri-ethanol amine (TEA) in the amounts of 2-5 mL/kg, improved yttria's dispersion.

### 3.2 Effect of Powder Particle Size

Interparticle spacing of yttria decreases by both steel and yttria particle diameter. A small *IPS* is desirable for efficient dispersion of yttria by ball milling; typically, it would take less time and energy to incorporate yttria into the steel matrix. From Eqn. (3), finer yttria is more effective in decreasing *IPS* than decreasing the steel powder's size. Also, the chromite layer on steel particles' surface makes it undesirable to work with very fine steel powder, as it would introduce too much oxygen into the system. Thus, it is critical to use very fine yttria to successfully process steels by mechanical alloying.

The calculated *IPS* may be taken as a measure of ease of mechanical alloying of a blended mixture. Otherwise, as mentioned in the introduction, observations made by atom probe tomography have established that yttria ought to dissociate and dissolve during mechanical alloying, and recombine on aging with titanium and excess oxygen to form yttrium titanate clusters that are an order of magnitude smaller than the yttria particles themselves, with a similar decrease in their *IPS,* to realize the full potential of ODS steels.

The intent of mechanical alloying for ODS processing is not so much to decrease particle size but to "knead" yttria into the steel matrix. Steel particles become flattened, break up, fold over and weld during processing, with no apparent decrease in their actual "particle size".

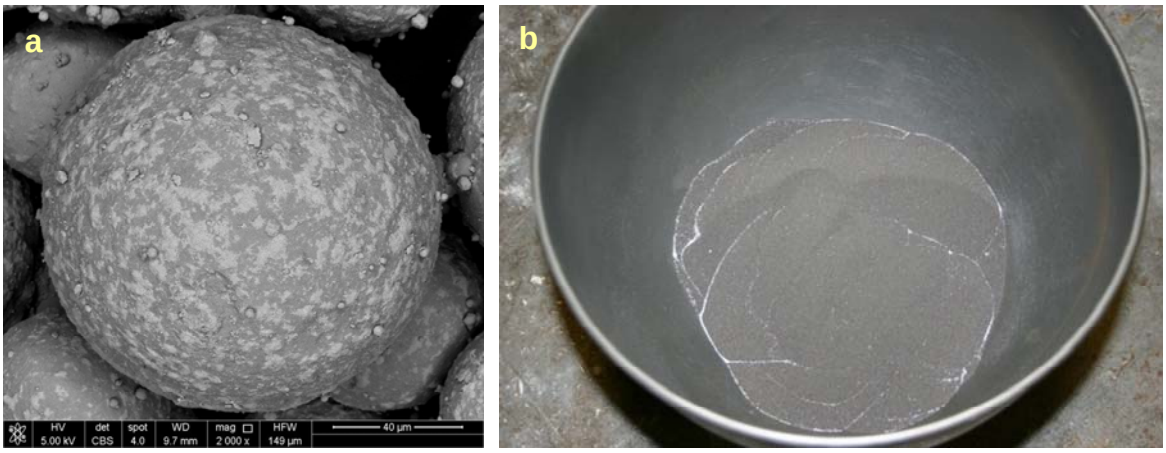


Fig. 2. From Batch M3 (a) SEM image of a steel powder coated with yttria on pre-mixing. (b) Streaks of excess yttria in a pre-mixing bowl that did not disappear even after very long mixing times.

### 3.3 Characterization of ODS Steels

A convenient way to check for dispersion strengthening is to check for an anticipated increase in hardness to levels above 400 HV. The microstructure would also consist of sub-micron grains. The extruded rods were sectioned at various locations along their length, and their hardness were measured (Table 3). None of the rods extruded outside showed a hardness range commensurate with ODS strengthening. Their microstructure consisted of coarse 10-20 µm ferrite grains with small islands of pearlite. A TEM study on Rod N5A could not find the presence of any Y-bearing dispersoids in the microstructure. Shavings were taken from rods for yttrium analysis by ICP. These results are also shown in Table 3. Presence of yttrium was not found in any significant quantity in these samples, except for the Rods N1, N2 and M7. However, these rods did not show dispersion strengthening either, and we were not able to explain what happened to yttrium in other rods.

The first evidence of oxide dispersion strengthening was seen in Rod M6A (Fig. 3). The ODS sections are more corrosion resistant than the casing steel because of their higher chromium content and could be easily distinguished by their contrast. They had hardness values exceeding 560 HV. Rod M6A was a F/M steel. Its chromium content provided high hardenability. It was feasible for martensite to form on exiting from the extrusion press. To investigate that possibility, the rod was double-tempered at 650°C and 720°C for 24 h each. It still retained much of its hardness at 490 HV. A tensile blank was cut from the rod, its mild steel casing was removed, and two parallel segments were machined for hardness traverses at quarter inch intervals (Fig. 3c). The measured hardnesses were consistently high, except on one side, a sharp drop-off was observed towards the end of the blank.

The extruded rods M4B, M7B and M9A were sectioned into tensile blanks and hardness blocks (Fig. 4). The transition behavior from hardened by dispersion strengthening to non-hardened steel

Table 5. Average Vickers hardness values (HV) of tensile blanks.

| Extruded Rod | Steel | Tensile blanks | | | | | |
|---|---|---|---|---|---|---|---|
| | | A | B | C | D | E | F |
| M4B | 14YWT | Soft | Transition | 369 | 362 | 357 | 367 |
| M7B | F/M Steel | Soft | Transition | 618 | Transition | Soft | |
| M9A | 14YWT | 426 | 419 | Transition | Soft | 420 | |

Hardness values were converted from HRC to HV for ease of comparison with Table 3.
Soft matrix is <20 HRC.

matrix was seen in these also. A summary of the hardness traverses made in these tensile blanks are given Table 5.

A TEM study was carried out on samples from Rod M6A in "As-extruded" and "Extruded and Tempered" condition. In some TEM views, a band of relatively coarse grains (Area 1) between sub-micron sized grains (Areas 2 and 3) were seen that also showed an absence of yttrium and titanium (Fig. 5).

Creep specimens were machined from tensile blanks shown in Table 5 to be tested at 750 and 700°C, 80 and 40 MPa. The first specimen M4B'C was placed in the creep frame in September 2015 to be tested at 750°C and 80 MPa, and the test is still running in steady state creep after 5000 h. Fig. 6 shows it in comparison to Japanese candidate SCWR fuel cladding materials, where their expected rupture life under the same conditions would have been 500 h.

## 4 Conclusions

Oxide dispersion strengthened (ODS) steels were prepared by mechanical alloying and consolidated by hot extrusion. Variable dispersion strengthening was found in the steels prepared as characterized by hardness testing and light microscopy; some steels did not show any strengthening, while others showed macroscopic transition from strengthened to non-strengthened areas. Such transitions were also observed in microscale by electron microscopy. Those steels that were adequately dispersion strengthened had creep strengths superior to austenitic stainless steels developed by Japan for their SCWR fuel cladding.

In mechanical alloying, a model was proposed to show the effect of yttria and steel powder size, and an optimum quantity of yttria required. It was shown that the finer the yttria and steel powder, the easier will yttria's dispersion into steel matrix be, with yttria particle size having the greater effect. A calculated yttria interparticle spacing ($IPS_Y$) was derived as a measure of ease of mechanical alloying of a blended mixture.

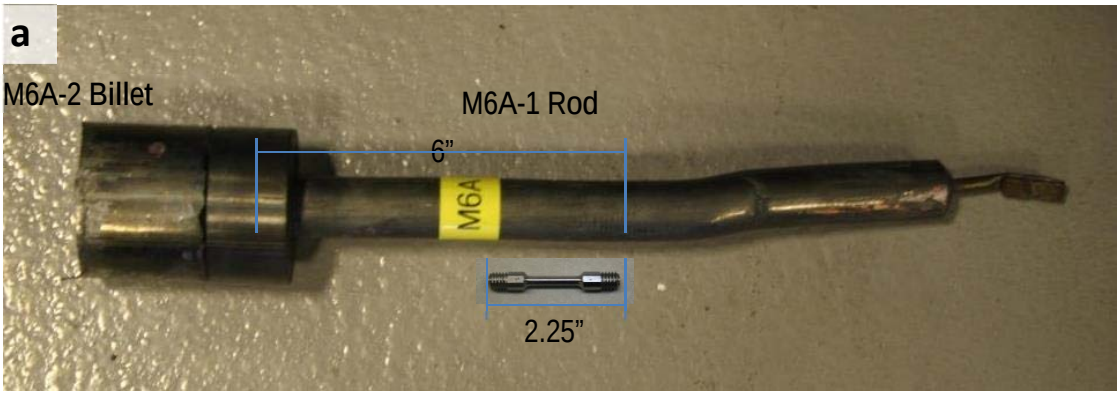


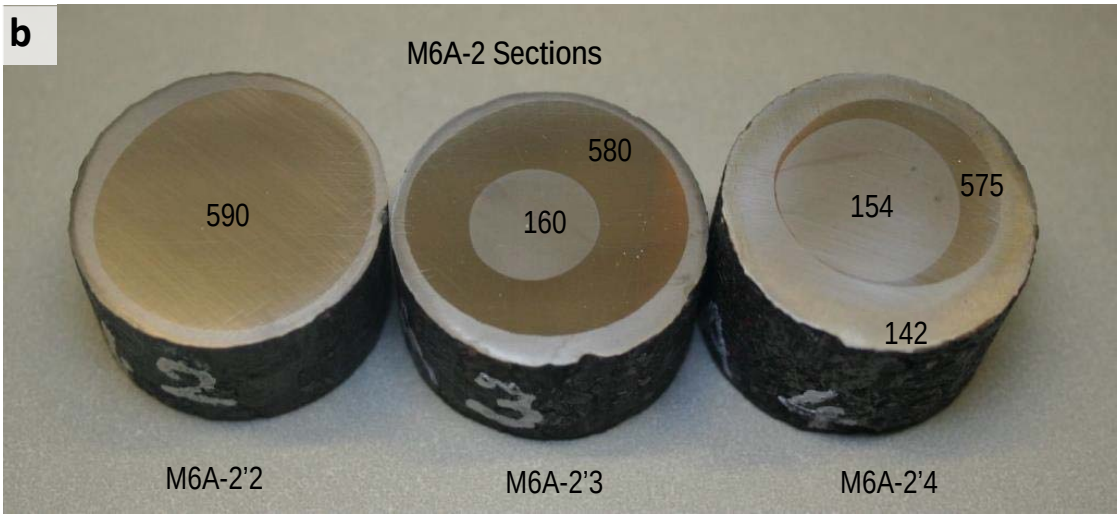


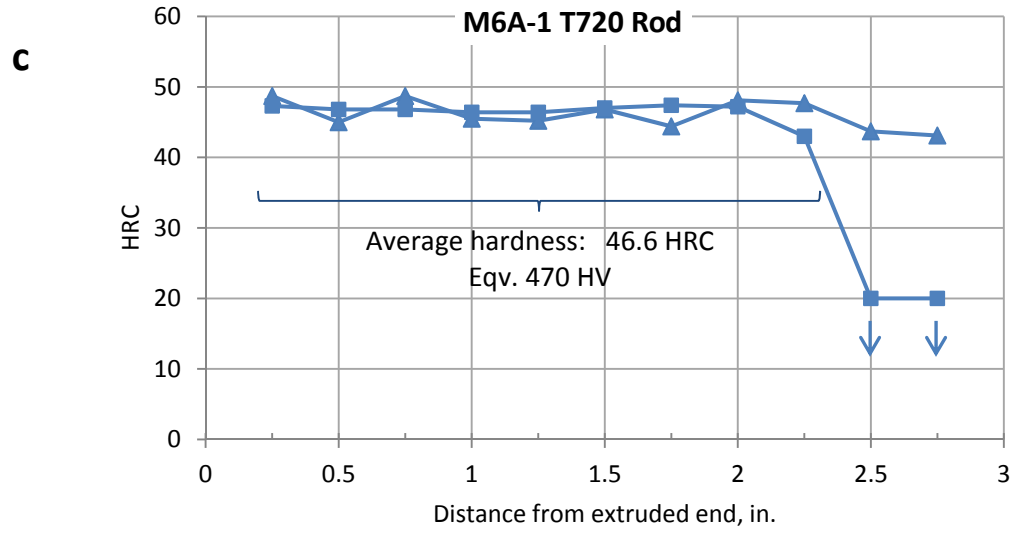


Fig. 3 (a) M6A-1 rod that stalled during extrusion. The extruded piece had high hardness ODS steel that resisted to softening on tempering at 650°C and 720°C for 24 h each. (b) Sections from M6A-2 rod with measured hardnesses in HV (5 kg-f, 15 s). (c) Hardness profile across the small-size tensile blank after two tempers at 650°C and 720°C.

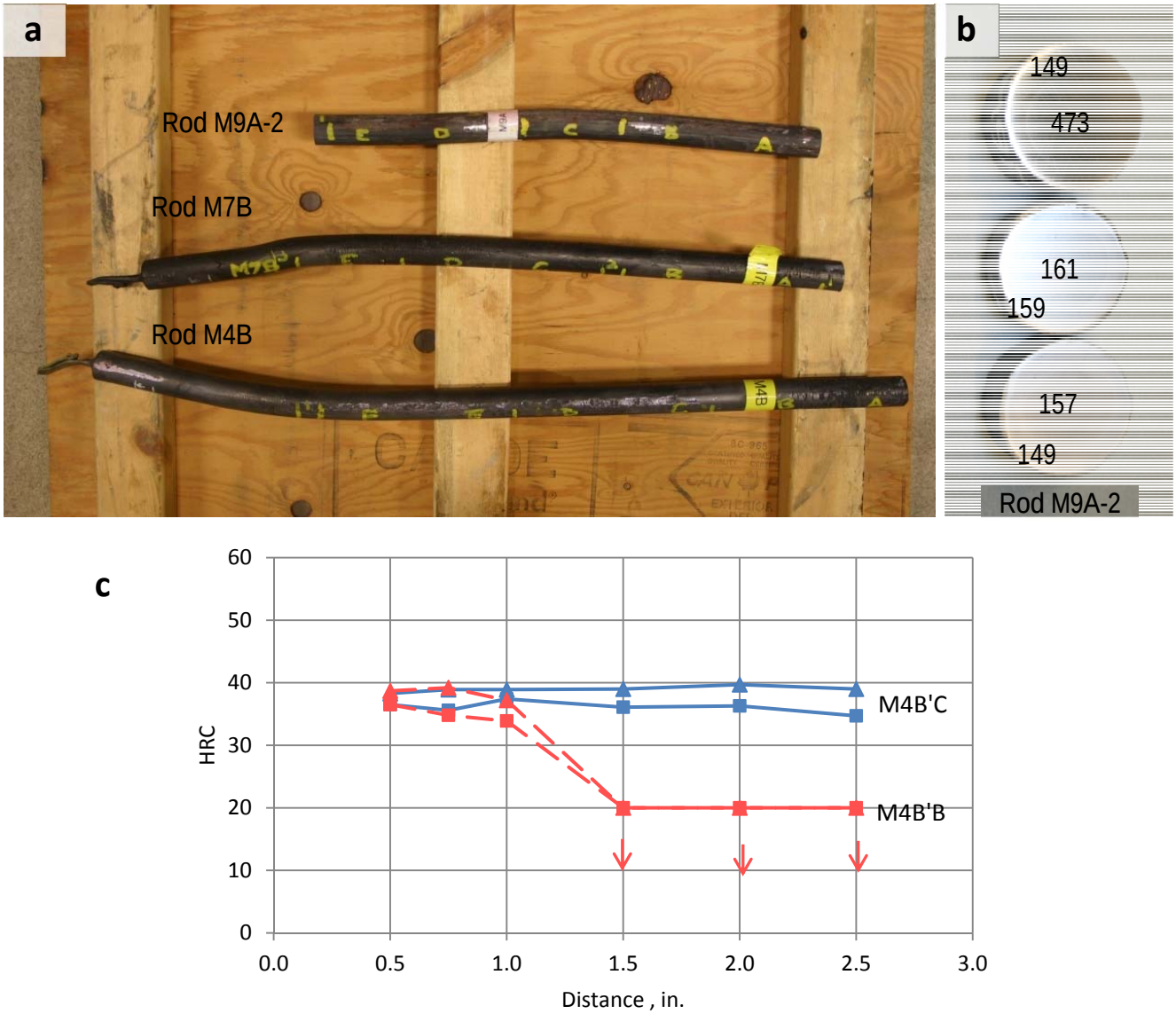


Fig. 4. (a) Rod M9A-2, M4B, M7B. (b) Sections from M9A-2 rod with measured hardnesses in HV (5 kg-f, 15 s). (c) Hardness profiles across two tensile blanks in Rod M4B, one showing a transition from ODS hardened to non-hardened steel matrix.

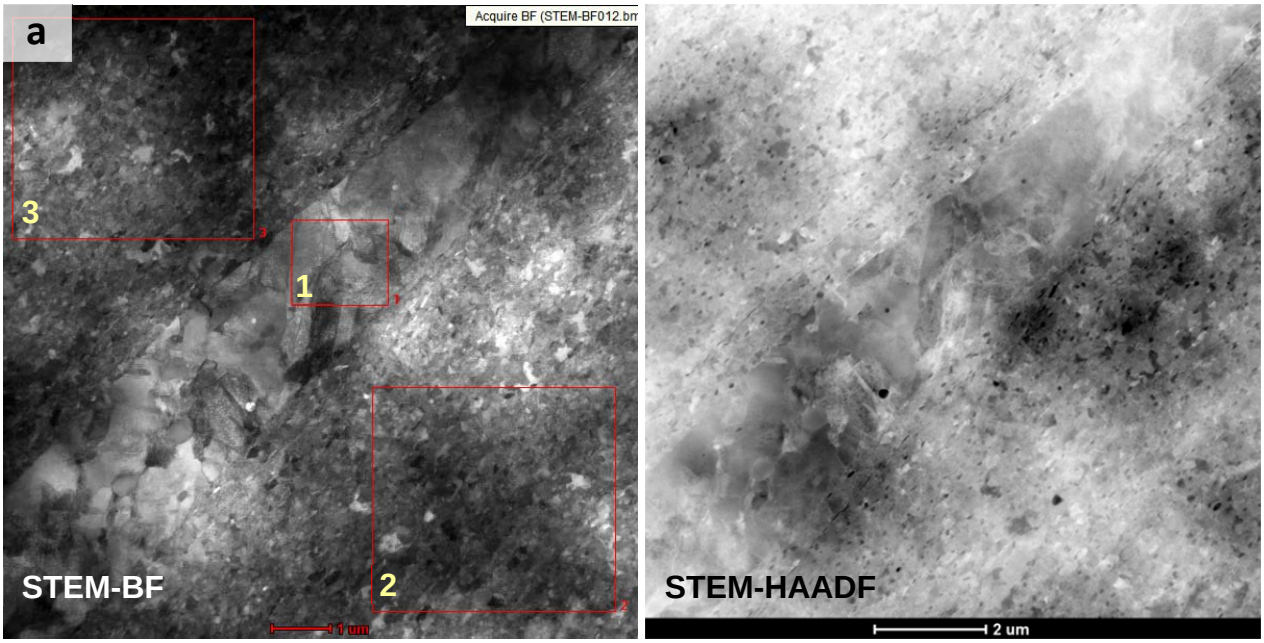


Chemical analysis of the selected areas (wt. pct.):

| | C | Cr | W | Y | Ti | Aver. grain size. (nm) | |
|---|---|---|---|---|---|---|---|
| Bulk | 0.11 | 9.6 | 2.2 | 0.28 | 0.9 | Before T | After T |
| Area 1 | | 6.7 | 1.6 | - | - | | 2000 |
| Area 2 | | 10.3 | 2.8 | 0.14 | 0.78 | 150 | 320 |
| Area 3 | | 10.6 | 2.7 | 0.17 | 0.92 | | |

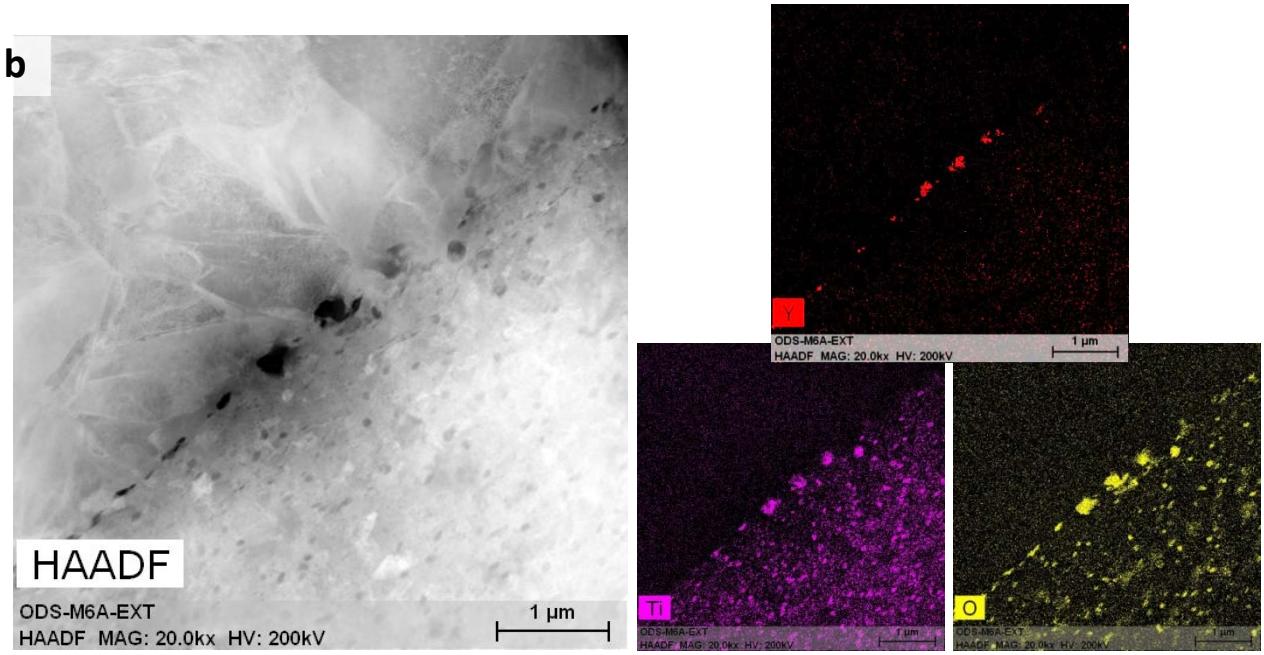


Fig. 5. Scanning TEM (STEM) study of sample from Rod M6A in "As-extruded" condition showing an area with micron-sized grains between areas with sub-micron-sized grains. (a) Yttrium was absent in the "coarse" grained region. (b) Boundary between Area 1 and Area 2 at a higher magnification. Y, Ti and O maps show larger yttrium titanate particles on the boundary and fine yttrium titanates in Area 2. (BF: Bright Field; HAADF: High Angle Annular Dark Field. T: Temper)

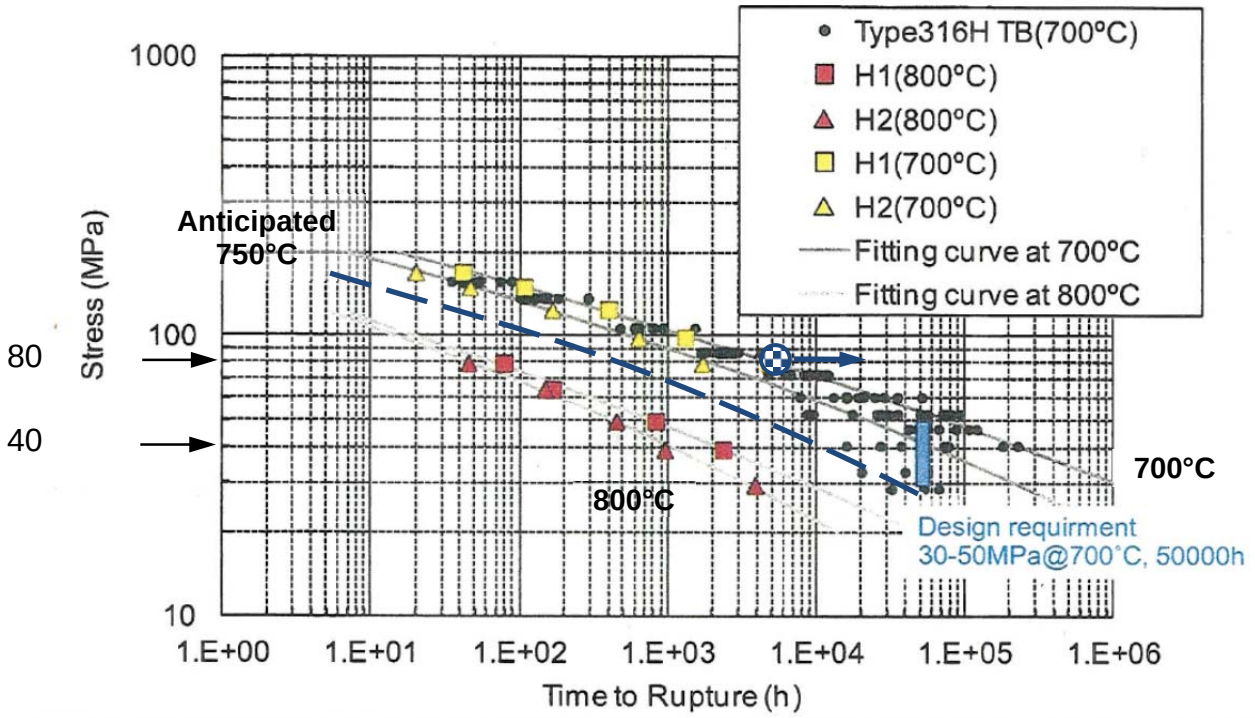


Fig. 6. Creep performance of ODS steel specimen M4B'C (being tested at 750°C, 80 MPa, still in steady state creep after 5,200 h – large checkered circle) in comparison to Japanese SCWR fuel cladding candidate materials, H1 and H2 austenitic steels. Japanese data from [14].

## 5 References

[1] Lee J S et al. (2007). "Embrittlement and hardening during thermal aging of high Cr oxide dispersion strengthened alloys", *J Nucl. Mater.* **367:**229-233.

[2] Serrano M et al. (2012). "Microstructural anisotropy effect on the mechanical properties of a 14Cr ODS steel", *J Nucl. Mater.* **428:**103–109.

[3] Alinger M J, Odette G R and Hoezler D T (2004). "The development and stability of Y-Ti-O nanoclusters in mechanically alloyed Fe-Cr based ferritic alloys", *J Nucl. Mater.* **333:**382-386.

[4] Larson D J et al. (2001). "3-D atom probe observation of nanoscale Ti-O clustering in an ODS Fe-12Cr-3W-0.4Ti + $Y_2O_3$ ferritic alloy", *Scripta Mater.* **44:** 359–364.

[5] Odette G R, Alinger M J and Wirth B D (2008). "Recent developments in irradiation-resistant steels", *Annual Rev. Mater. Res.* **38:** 471-503.

[6] Ukai S et al. (1993). "Alloying design of ODS ferritic steel for long life Fast Breeder Reactor core materials", *J Nucl. Mater.* **204:**65-73.

[7] Ribis J and Carlan Y de (2012). "Interfacial strained structure and orientation relationships of the nanosized oxide particles deduced from elasticity-driven morphology in ODS materials", *Acta Mater.* **60:**238–252.

[8] Alinger M J, Odette G R and Hoelzer D T (2009). "On the role of alloy composition and processing parameters in nanocluster formation and dispersion strengthening in nanostuctured ferritic alloys", *Acta Mater.* **57:**392–406.

[9] Miller M K, Russell K F and Hoelzer D T (2006). "Characterization of precipitates in MA/ODS ferritic alloys", *J. Nucl. Mater.* **351:**261–68.

[10] Dawson K and Tatlock G (2014). "Characterisation of nanosized oxides in ODM401 oxide dispersion strengthened steel", *J Nucl. Mater.* **444:**252–260.

[11] Sakasegawa H et al. (2011). "Stability of non-stoichiometric clusters in the MA957 ODS ferrtic alloy", *J Nucl. Mater.* **417:**229–232.

[12] Sakasegawa H et al. (2009). "Correlation between chemical composition and size of very small oxide particles in the MA957 ODS ferritic alloy", *J Nucl. Mater.* **384:**115–118.

[13] Bibby C and Kuyucak S (2010). "Estimation of particle size of yttria ($Y_2O_3$) powder procured from overseas", MTL 2010-18 (TR-R), (2010 Apr 7).

[14] Kaneda J et al. (2011). "Material development for SCWR", *Proc. 5th Int. Symp. SCWR,* Vancouver, BC, 2011 Mar 13-16.